Supplementary Materials for:

Aldehyde Dehydrogenase 1a1 Mediates a GABA Synthesis Pathway in Midbrain Dopaminergic Neurons

Jae-Ick Kim[1], Subhashree Ganesan[1], Sarah X. Luo[2,3], Yu-Wei Wu[1], Eric J. Huang[2,4], Lu Chen[1], and Jun B. Ding[1,5] *

[1]Department of Neurosurgery, Stanford University School of Medicine

[2]Department of Pathology, [3]Neuroscience Graduate Program, University of California San Francisco, San Francisco, CA 94143 [4]Pathology Service 113B, San Francisco VA Medical Center, San Francisco, CA 94121

[5]Department of Neurology and Neurological Sciences, Stanford University School of Medicine, Palo Alto, CA 94304, USA

This PDF file includes:

Materials and Methods:

Animals

Adult (8-12 weeks, male and female) mice were used for this study. DAT-Cre (B6.SJL-*Slc6a3*$^{tm1.1(cre)Bkmn}$/J, JAX stock number 006660) or A2A-Cre mice (B6.FVB(Cg)-Tg(Adora2a-cre)KG139Gsat/Mmucd, MMRRC stock number 036158-UCD) were crossed with Ai32 mice (*40*) (B6;129S-*Gt(ROSA)26Sor*$^{tm32(CAG-COP4*H134R/EYFP)Hze}$/J, JAX stock number 012569) to produce DAT-Cre;Ai32 or A2A-Cre;Ai32 mice. A2A-Cre;Ai32 mice were further bred with Drd1a-tdTomato mice (B6.Cg-Tg(Drd1a-tdTomato)6Calak/J, JAX stock number 016204) to generate A2A-Cre;Ai32; Drd1a-tdTomato mice. DAT-Cre;Ai32 or A2A-Cre;Ai32;Drd1a-tdTomato mice were crossed with GAD1fl/fl;GAD2fl/fl mice (obtained from Dr. Richard Palmiter's lab) to generate DAT-Cre;Ai32;*Gad1*fl/fl;*Gad2*fl/fl or A2A-Cre;Ai32;Drd1a-tdTomato;*Gad1*fl/fl;*Gad2*fl/fl mice. *Aldh1a1*-/-;DAT-Cre;Ai32; or *Aldh1a1*-/-;A2A-Cre;Ai32;Drd1a-tdTomato mice were generated by crossing DAT-Cre;Ai32 and A2A-Cre;Ai32;Drd1a-tdTomato mice with *Aldh1a1*-/-mice (B6.129-*Aldh1a1*^{tm1Gdu}/J, JAX stock number 012247). All experimental procedures were conducted in accordance with protocols approved by Stanford University's Administrative Panel on Laboratory Animal Care.

Brain slice preparation

Oblique horizontal or coronal brain slices (300 µm) containing the dorsal striatum, or nucleus accumbens were obtained using standard techniques (*41*). Mice were anesthetized with isoflurane, decapitated, and briefly exposed to chilled artificial cerebrospinal fluid (ACSF) containing 125 mM NaCl, 2.5 mM KCl, 1.25 mM NaH_2PO_4, 25 mM $NaHCO_3$, 15 mM glucose, 2 mM $CaCl_2$ and 1 mM $MgCl_2$ oxygenated with 95% O_2 and 5% CO_2 (300~305 mOsm, pH 7.4). Acute brain slices containing dorsal striatum were prepared using a tissue vibratome and slices were first maintained in ACSF for 30 min at 34 °C and then for another 30 min at room temperature. For drug studies, brain slices were incubated with each inhibitor for 2~4 hours and the same inhibitor was applied throughout the recording session. After recovery, slices were transferred to a submerged recording chamber perfused with ACSF at a rate of 2~3 ml/min at 30~31 °C and brain slices were recorded within 4 hours after recovery. For DEAB, Disulfiram, SNAP-5114, RA, Sulpride, and GBR12935, stock solution was made in DMSO, then diluted 1:1000 in ACSF to the final concentration. In the controls, the same concentration of DMSO was included in ACSF for incubation and perfusion.

Electrophysiology, optogenetic stimulation and pharmacology

Spiny projection neurons were visually identified by conventional IR-DIC optics. Whole-cell voltage clamp recordings were made with borosilicate glass pipettes (2.5~3.5 MΩ) filled with an Cs^+-based low Cl^- internal solution containing 126 mM $CsMeSO_3$, 10 mM HEPES, 1 mM EGTA, 2 mM QX-314 chloride, 0.1 mM $CaCl_2$, 4 mM MgATP, 0.3 mM Na_3GTP, 8 mM Na_2-phosphocreatine (280~290 mOsm, pH 7.3 with CsOH). To measure both oIPSC and oEPSC from the same SPN neurons, Membrane potentials were first held at +8 mV (the reversal potential of ionotropic glutamate receptors, liquid junction potential not corrected) to measure oIPSC and then continuously held at –70 mV (the reversal potential of chloride) to measure oEPSC. To stimulate ChR2-expressing axons from DA neurons, blue laser light (450 nm, 0.5 msec pulses with 60 sec intervals, saturation power under the objective less than 20 mW, was focused on the back focal plane of the objective to produce wide-field illumination. Access resistance was 10~20 MΩ (no compensation) and only cells with a change in access resistance < 20% were included in the analysis. Whole-cell patch recordings were performed using Multiclamp 700B and signals were filtered at 2 kHz and digitized at 10 kHz. Recording data were monitored and analyzed offline using Clampfit 10.0.

To examine synaptic responses following ChR2 stimulation, we performed whole-cell voltage-clamp recordings with low-chloride internal solution (E_{Cl} =~-70 mV, chloride reversal potential) from identified dorsal striatal SPNs. ChR2 stimulation evoked fast, monosynaptic, optogenetically-evoked excitatory post synaptic currents (oEPSCs) in all SPNs (held at -70 mV). oEPSCs were completely blocked with NBQX (AMPAR blocker, 10 μM) and R-CPP (NMDAR blocker, 10 μM). Optogenetically-evoked IPSCs (oIPSCs) were recorded in all SPNs (held at +8 mV, liquid junction potential uncompensated), and were completely abolished by $GABA_A$ receptor ($GABA_AR$) antagonist (SR95531, 10 μM) (fig. S2).

To test if blocking GAD enzyme function abolished GABA release, we used GAD blocker 3-mercaptopropionic acid (3-MPA, 500 μM, incubation for 30 min to 4 hours)(*42*). To ensure 3-MPA successfully blocked GABA synthesis, we recorded dSPNs in A2A-Cre;Ai32;D1-tdTomato mice, where Cre recombinase expression in A2A-Cre mice is controlled by the adenosine A2A receptor promoter (*43*) In these mice, ChR2 is selectively expressed in iSPNs but not midbrain dopaminergic neurons. tdTomato expression is essential for identifying dSPNs, which will not express ChR2. oIPSCs recorded in dSPNs by optogenetic stimulation of iSPNs were significantly attenuated by 3-MPA. After 45-60 min incubation with 3-MPA, we started to observe a reduction of conventional GABA release, and inhibition was nearly saturated at ~ 2 hours. As 4 hours of incubation caused only a ~10% further reduction in oIPSC amplitude, we

grouped data after 2-4 hours incubation.

To test if blocking DAO and ALDH reduces GABA release, we used DAO inhibitors: aminoguanidine, (AG 100 μM) or amiloride (10 μM) (*15, 44*), and ALDH inhibitors: 4-(diethylamino)-benzaldehyde (DEAB, 10 μM), or disulfiram (10 μM) (*21, 45*).

Blockade or genetic deletion of ALDH1a1 does not completely abolish GABA co-release, as ~30% residual GABA co-release remains in *Aldh1a1*-/- mice. This prompts the question of what else can contribute to GABA accumulation in midbrain DA neurons. DA neurons can take up extracellular GABA through GABA transporters (GAT1 and GAT3) in order to sustain GABA transmission (*7*). We also observed this effect using a combination of GAT1 (NNC-711, 4 μM) and GAT3 (SNAP-5114, 50 μM) blockers, which almost completely abolished the remaining GABA co-release in *Aldh1a1*-/-;DAT-Cre;Ai32 mice (fig. S11). This finding suggests that GABA transporters also contribute to the accumulation of pre-synaptic GABA in midbrain DA neurons.

For all prolonged EtOH treatments, brain slices from either hemisphere were randomly assigned to control (treated with ACSF) or EtOH treatment (EtOH) groups, and recordings were alternated between control and EtOH treatment groups. The incubation and perfusion solutions in the EtOH treatment group contained the same EtOH concentration. To mimic the blood alcohol levels of binge drinking, we pretreated striatal brain slices for 2-4 hours (same time course as the 3-MPA treatment to target conventional GABA synthesis) with 17-50 mM EtOH (17 mM is equivalent to 0.08 wt/vol, the legal blood alcohol concentration limit in the U.S. at which people are allowed to drive cars).

For *in vivo* EtOH repeated administration, mice were injected daily with EtOH (2 g/kg, 20%, intraperitoneal injection) for consecutive 7 days to approximate binge drinking episodes in humans (*31*). Mice in the control groups received equivalent injections of saline. Two to four hours after the final EtOH injection, striatal brain slices were prepared from DAT-Cre;Ai32 mice and record oIPSCs in SPNs. During incubation and recording, we did not include EtOH in the perfusion solution.

Stereotaxic viral injection

Stereotaxic virus injections were conducted on P35~P49 male and female DAT-Cre;Ai32, *Aldh1a1*-/-;DAT-Cre;Ai32, and C57BL6/J mice. Before surgery, mice were deeply anesthetized by intraperitoneal injection of ketamine (100 mg/kg) / xylazine (10 mg/kg) solution. A total volume of 950 nl virus solution (AAV control, knock-down, and rescue) was injected bilaterally into Substantia Nigra pars compacta (coordinates used, AP: -3.1 mm, ML: ±1.2 mm from bregma, DV: -4.0 mm from exposed dura mater). A glass micropipette with a long narrow tip

(size: 10~20 μm) was pulled using a micropipette puller to deliver virus. The glass pipette was slowly lowered to target area and left for 10 min before virus injection. Virus solution was injected at an infusion rate of 100 nl/min and withdrawn 10 min after the end of injection. Following virus injection, the scalp was sutured and mice were returned to their home cages. Virus-injected mice were used for experiment at least 2 weeks after virus infusion.

In Situ Hybridization

RNA probes for in situ hybridization were prepared using plasmids that contained cDNA for mouse GAD67 (obtained from Dr. David Lewis, cited in Curley et. al., 2013, Nerobiol. Dis.) and human GAD65 (obtained from Prof. David Rowitch). The plasmids were linearized with appropriate restriction enzymes, and transcribed with SP6, T7 or T3 polymerase using digoxigenin (DIG) RNA labeling kit. Mice were transcardially-perfused with 4% PFA in DEPC-treated PBS. Brains were removed and fixed overnight in 4% PFA in DEPC-treated PBS, cryoprotected in 15% and 30% DEPC-treated sucrose and embedded in OCT. Free-floating sections were prepared at 40μm. Sections were incubated with hybridization buffer containing DIG-labeled riboprobes (200 ng/ml) at 65°C overnight. The next day, sections were either processed for alkaline phosphatase color reaction using BM purple or developed for fluorescent signal using the TSA Plus DNP (HRP) System and using the Cyanine 3 tyramide reagent.

Immunohistochemistry

For immunofluorescence staining, sections were incubated with anti-tyrosine hydroxylase antibody (1:1000, ab152), anti-aldehyde dehydrogenase 1a1 (1:200, ab195254, Abcam), and anti-GFP (1:1000, ab5450) at 4 °C overnight, followed by secondary antibodies conjugated to Alexa 488, Alexa 594 or Alexa 647 fluorophores at room temperature for 1 hour to detect signals. For chromogenic staining, sections were incubated with primary antibody overnight, followed by incubation with biotinylated IgG and avidin-biotin complex (Vector Laboratories). DAB solution was used to visualize expression. Images were captured using a confocal microscope or a microscope equipped with a CCD camera.

Raldh1-shRNA generation and AAV preparation

Five different shRNAs targeting different regions of mouse *aldh1a1* were cloned into the lentiviral vector pJHUG (*46*), which expressed shRNA under the H1 promoter and GFP under ubiquitin promoter to label infected cells. Knock-down efficiency was tested by co-transfection of *Aldh1a1*-egfp and the shRNA constructs into HEK293 cells and analyzing lysates by western

blot against GFP. To further confirm knock-down efficiency of endogenous *Aldh1a1* in neurons, dissociated mouse hippocampal neurons were infected with lentivirus containing shRNA construct or empty vector. cDNA from neurons were analyzed by real-time PCR using *aldh1a1* Taqman probe (Mm00657317_m1, Applied Biosystems) an actin B probe (4352933E, Applied Biosystems). Relative expression level of *Aldh1a1* was calculated using the ΔΔCt method. The sequence of shRNA used in this study was GGCACTCAATGGTGGGAAATTCAAGAGA-TTTCCCACCATTGAGTGCC. For the rescue construct, the *Aldh1a1* coding region was PCR amplified from mouse hippocampal cDNA. shRNA resistant *Aldh1a1* was made by inducing six silent mutations in the shRNA binding region and expressed with a C-terminal EGFP tag under the ubiquitin promoter in the rescue construct. For *in vivo* studies, we used Adeno Associated virus (AAV) to get higher infectivity. AAV vector described previously (*47*), was a generous gift from the Südhof laboratory. The vector backbone consisted of the ApaI-XbaI fragment from the lentiviral construct containing the H1 promoter; the shRNA was cut and inserted into the AAV vector backbone. EcoR1-BsRG1 fragment containing *Aldh1a1*-egfp was inserted into the AAV vector downstream of the CMV promoter to create the rescue construct. AAV was prepared as described previously (*47, 48*). Briefly, AAV vectors were co-transfected with pDJ and pHelper into HEK-293 cells. After 72 hours, cells were collected, lysed and AAV was purified by using an iodixanol gradient.

Mouse behavior tests

Open-field test: Mice were placed in a 40 cm (L) X 40 cm (W) X 40 cm (H) open-field chamber. Locomotor activity was recorded for 10 minutes using an overhead digital camera. The mouse position in the open field was tracked using Viewer. Two-bottle choice test: To test the consequence of ALDH1a1 deletion on EtOH intake, we used home cage continuous two-bottle choice test to examine voluntary EtOH consumption in *Aldh1a1*-/- mice and their WT lit-termates, or C57BL6/J mice injected with control, *Aldh1a1* KD, and rescue viruses (*33, 49, 50*). *Aldh1a1*+/+, *Aldh1a1*-/- (male and female, 8 weeks, C57BL6/J background), and C57BL6/J mice (male and female, 8 weeks) injected bilaterally with 3 different viruses (AAV-GFP, AAV-shRNA, AAV-shRNA-aldh1a1*, also see fig.S9) were individually housed and acclimated for one week prior to beginning the test. Two-bottle choice test consisted of 3 cycles of four days each: First, individually housed mice were presented with two water bottles located in two different positions in the home cage. After four days, one water bottle was replaced by 3% EtOH (v/v in tap water) bottle for four days. For the 3rd cycle of the test, a 3% EtOH bottle was replaced by a 10% EtOH bottle for another 4 days. Positions of the bottles (water vs. ethanol) were switched

every 2 days to prevent side preference. Daily ethanol consumptions were measured at 1800 h by weighing the bottles and the mice were weighed once a week. Preference ratio for ethanol is calculated as ethanol volume / total volume consumed.

Data and statistical analysis

All the data were analyzed using Clampfit 10.0, Origin 8 and ImageJ. Statistical analysis was conducted using Prism 5. Summary graphs were all shown as mean ± SEM. Unpaired student t-test, one-way ANOVA with post-hoc Newman-Keuls comparison test, repeated measures 2-way ANOVA with post-hoc Bonferroni test were used to determine statistical difference among treatment groups. $P < 0.05$ was considered statistically significant. Measured values and statistical test used illustrated in main figures were summarized in Table S1.

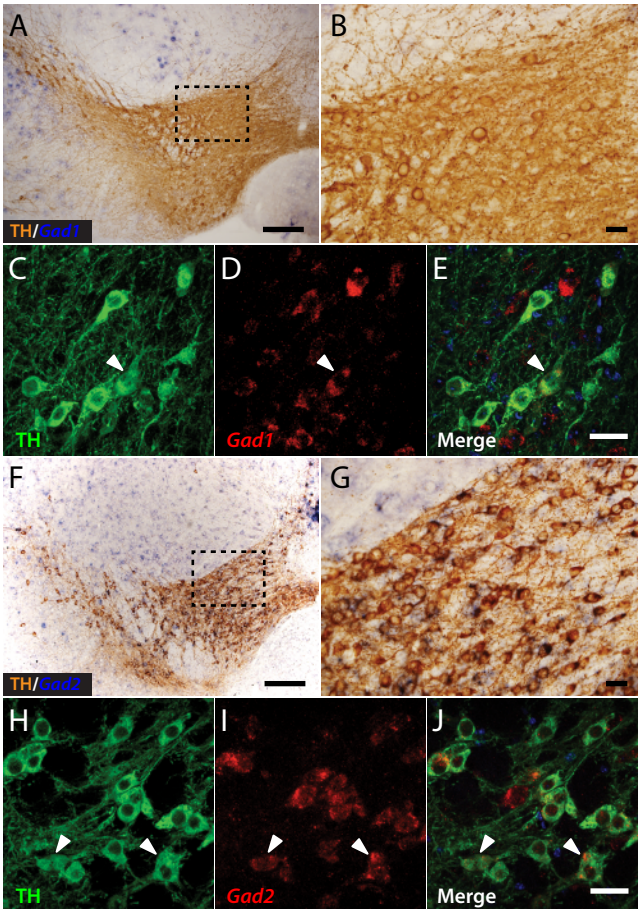

fig. S1. GAD1 and GAD2 expression in VTA

(A to J) Expression of *Gad1* and *Gad2* mRNA in DA neurons of the VTA. Low (A and F) and high (B and G) magnification images of immunolabeled tyrosine hydroxlase (TH)-positive dopaminergic neurons show little colocalization with *Gad1* (A and B) and *Gad2* (F and G) mRNA, detected using chromogenic in situ hybridization (ISH). Confocal images of fluorescence ISH for *Gad1* (D) and *Gad2* (I) mRNA (red) combined with TH immunolabeling (green C and H) confirm that few TH+ neurons express *Gad1* or *Gad2* in the VTA. In SNc, *Gad1*+:TH+ / Total TH+ neurons = 8.7 ± 0.9 %; n = 704 neurons quantified; *Gad2*+:TH+ / Total TH+ neurons = 8.78 ± 0.97 %; n = 660 neurons quantified, N = 3 animals, 4 serial sections from each; In VTA, *Gad1*+:TH+ / TH+ = 13.8 ± 3.2 %; n = 377 neurons; *Gad2*+:TH+ / TH+ = 18.4 ± 5.6 %; n = 353 neurons, N = 3 animals, 4 serial sections from each. Scale bars: 200 µm for A,F, 50 µm for B-E, G-J.

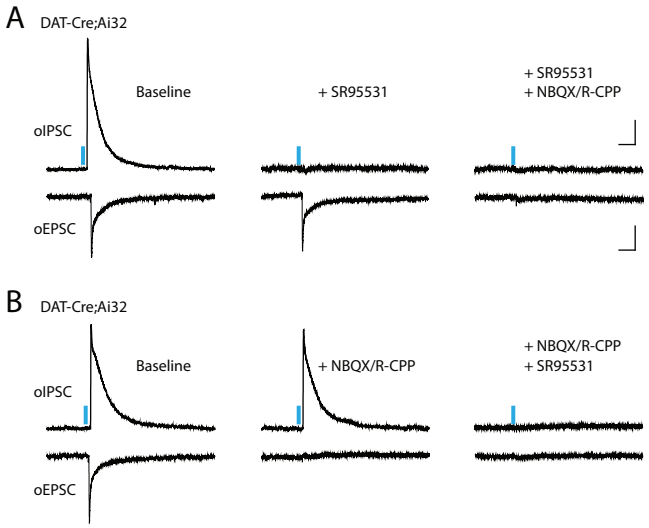

fig. S2. Midbrain dopaminergic neurons co-release GABA and glutamate.
(A) Evoked oIPSC and oEPSC from an SPN to optogenetic stimulation of dopaminergic axons upon sequential application of $GABA_A$ receptor blocker, SR95531 (10 μM) and cocktail of AMPA/NMDA receptor blockers, NBQX (10 μM)+R-CPP (10 μM). (B) Another example of evoked oIPSC and oEPSC with blockers applied in reverse order. oIPSC and oEPSC were caused by direct activation of ionotropic GABA and glutamate receptors in SPNs. Blue rectangular bar indicates 450 nm light stimulation. Scale bars represent 200 pA, 100 ms for oIPSC and 50 pA, 100 ms for oEPSC.

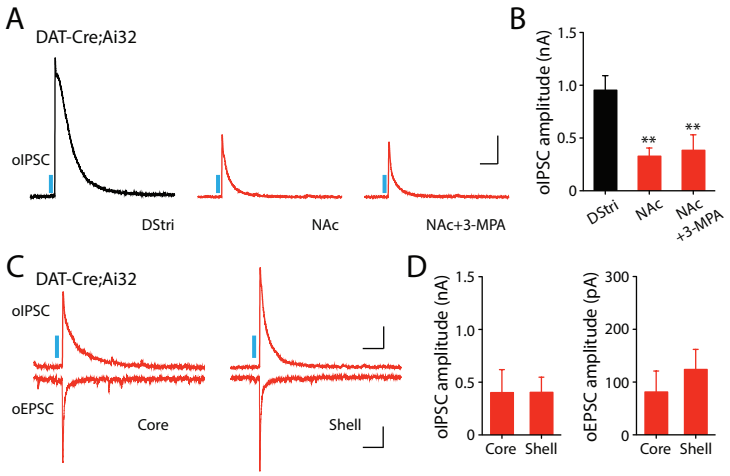

fig. S3. GABA co-release in the dorsal striatum and the nucleus accumbens (NAc).
(A) Representative oIPSC recording traces from dorsal striatum (DStri) and NAc in DAT-Cre;Ai32 mice treated with 3-MPA (500 μM). (B) Summary statistics for oIPSC (DStri, 0.95 ± 0.14 nA, n = 5 cells; NAc, 0.33 ± 0.08 nA, n = 15 cells; NAc treated with 3-MPA, 0.38 ± 0.15 nA, n = 6 cells; $F_{2, 23} = 7.623$, $P < 0.01$, one-way ANOVA with post-hoc Newman Keuls comparison test; DStri vs NAc, $P < 0.01$; DStri vs NAc plus 3-MPA, $P < 0.01$). Scale bars represent 200 pA, 100 ms for oIPSC. (C) Representative oIPSC and oEPSC recording traces from NAc core and NAc shell regions in DAT-Cre;Ai32 mice. (D) Summary statistics for oIPSC (core, 0.40 ± 0.22 nA, n = 4 cells; shell, 0.40 ± 0.14 nA, n = 5 cells; $P > 0.05$, unpaired t-test) and for oEPSC (core, 81.34 ± 39.59 pA, n = 4 cells; shell, 123.90 ± 38.07 pA, n = 5 cells; $P > 0.05$, unpaired t-test). Blue rectangular bar indicates 450 nm light stimulation. Scale bars represent 100 pA, 100 ms for oIPSC and 25 pA, 100 ms for oEPSC. Mean ± SEM is used for all the data described in the figure.

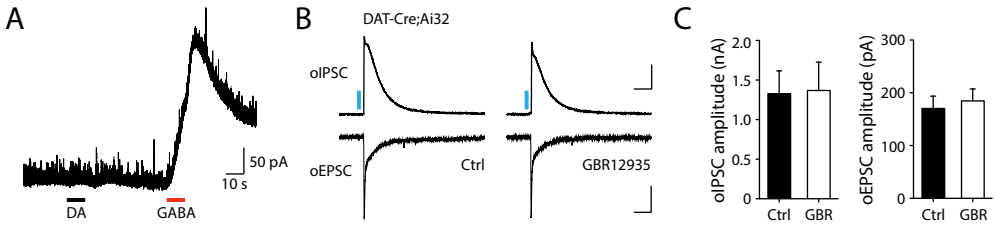

fig. S4. DA does not directly influence dopaminergic oIPSC and oEPSC.
(A) Current response from an SPN held at 8 mV. Local application of DA (3 mM) does not directly activate $GABA_A$ receptor; while in the same neuron GABA (10 μM) evoked an IPSC. (B) Representative oIPSC and oEPSC recording traces in DAT-Cre;Ai32 mice treated with DA transporter blocker GBR12935 (50 nM). (C) Summary statistics for oIPSC (control, 1.33 ± 0.29 nA, n = 5 cells; GBR12935, 1.37 ± 0.36 nA, n = 6 cells; P > 0.05, unpaired t-test) and for oEPSC (control, 170.30 ± 23.43 pA, n = 4 cells; GBR12935, 184.70 ± 22.67 pA, n = 6 cells; P > 0.05, unpaired t-test). Blue rectangular bar indicates 450 nm light stimulation. Scale bars represent 400 pA, 100 ms for oIPSC and 50 pA, 100 ms for oEPSC. Mean ± SEM is used for all the data described in the figure.

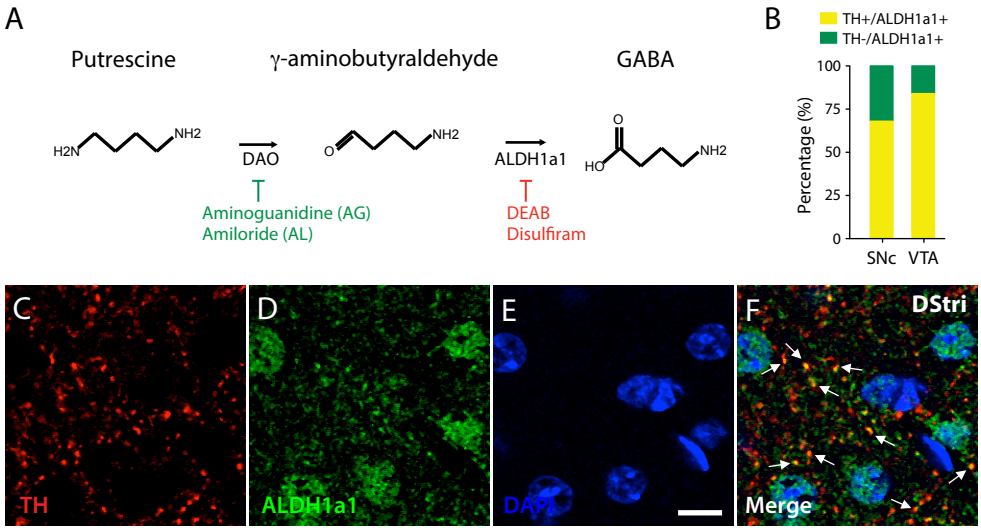

fig. S5. Quantification of TH+/ALDH1a1+ neurons in midbrain DA neurons and **ALDH1a1 expression in the dorsal striatum.**
(A) Non-canonical GABA synthesis pathway. GABA is biosynthesized from putrescine via a 2-step conversion process catalyzed by diamine oxidase (DAO) and aldehyde dehydrogenase (ALDH1a1). DAO can be inhibited by amiloride and aminoguanidine (AG), and ALDH activity can be blocked by DEAB and disulfiram. (B) Quantification of TH expression in ALDH1a1+ DA neurons in SNc and VTA. In SNc, TH+:ALDH1a1+ / Total ALDH1a1+ neurons = 67.6 ± 6.9 %; n = 357 neurons quantified, 11 slices from 2 animals. In VTA, TH+:ALDH1a1+ / Total ALDH1a1+ neurons = 84.1 ± 6.3 %; n = 124 neurons quantified, 7 slices from 2 animals. (C to F) Confocal images depicting double immunostaining for TH (C, red), ALDH1a1 (D, green), and DAPI (E, blue) in the dorsal striatum. (F) Merged confocal image, arrows depict co-localization of TH and ALDH1a1 in striatal dopaminergic terminals. Scale bar: 10 μm.

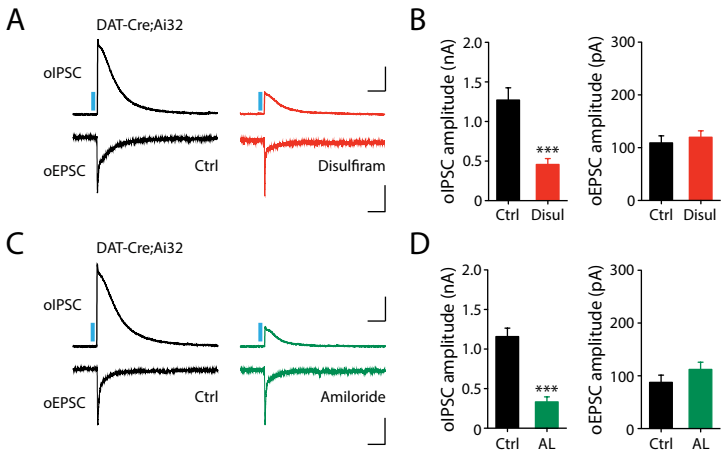

fig. S6. ALDH1 and DAO specific inhibitors selectively reduce dopaminergic oIPSC.
(A) Representative oIPSC and oEPSC recording traces in DAT-Cre;Ai32 mice treated with disulfiram (10 μM). (B) Summary statistics for oIPSC (control, 1.27 ± 0.16 nA, n = 17 cells; disulfiram, 0.46 ± 0.07 nA, n = 13 cells; $P < 0.001$, unpaired t-test) and for oEPSC (control, 109.20 ± 13.28 pA, n = 17 cells; disulfiram, 119.80 ± 12.21 pA, n = 11 cells; $P > 0.05$, unpaired t-test). Data used for control group are the same control used in Fig. 2F. (C) Representative oIPSC and oEPSC recording traces in DAT-Cre;Ai32 mice treated with amiloride (10 μM). (D) Summary statistics for oIPSC (control, 1.16 ± 0.11 nA, n = 12 cells; amiloride, 0.33 ± 0.06 nA, n = 12 cells; $P < 0.001$, unpaired t-test) and for oEPSC (control, 87.62 ± 13.65 pA, n = 11 cells; amiloride, 112.20 ± 13.53 pA, n = 11 cells; $P > 0.05$, unpaired t-test). Data used for control group are the same control used in Fig. 2H. Blue rectangular bar indicates 450 nm light stimulation. Scale bars represent 400 pA, 100 ms for oIPSC and 50 pA, 100 ms for oEPSC. Mean ± SEM is used for all the data described in the figure.

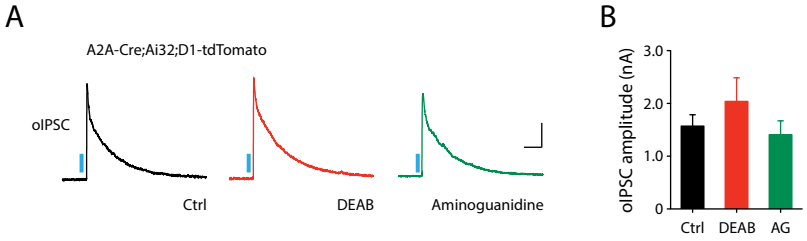

fig. S7. ALDH1 and DAO specific inhibitors do not affect conventional intrastriatal GABAergic transmission between SPNs.
(A) Representative oIPSC recording traces in A2A-Cre;Ai32;Drd1a-tdTomato mice treated with DEAB (10 μM) and aminoguanidine (100 μM). (B) Summary statistics for oIPSC (control, 1.57 ± 0.22 nA, n = 7 cells; DEAB, 2.04 ± 0.45 nA, n = 5 cells; aminoguanidine, 1.41 ± 0.26 nA, n = 5 cells; $F_{2, 14} = 1.044$, $P > 0.05$, one-way ANOVA). Blue bar indicates 450 nm light stimulation. Scale bars represent 400 pA and 100 ms for oIPSC. Mean ± SEM is used for all the data described in the figure.

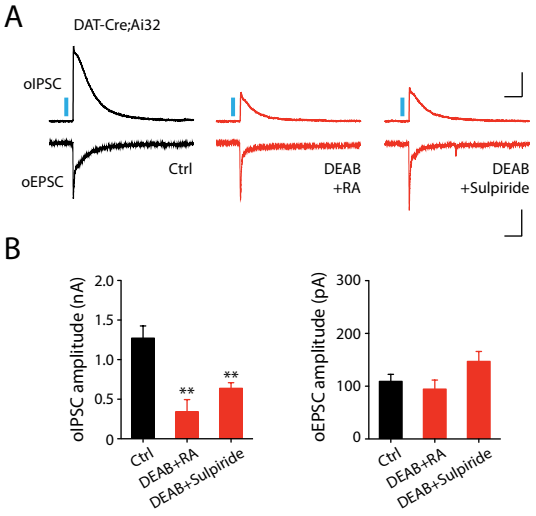

fig. S8. The effect of DEAB on dopaminergic oIPSC is not caused by either deficit in retinoic acid (RA) synthesis or DA D2 auto-receptor activation.

(A) Representative oIPSC and oEPSC recording traces in DAT-Cre;Ai32 mice treated with DEAB plus either RA (1 μM) or DA D2 receptor antagonist sulpiride (10 μM). (B) Summary statistics for oIPSC (control, 1.27 ± 0.16 nA, n = 17 cells; DEAB plus RA, 0.34 ± 0.15 nA, n = 5 cells; DEAB plus sulpiride, 0.64 ± 0.07 nA, n = 14 cells; $F_{2, 33} = 10.12$, $P < 0.001$, one-way ANOVA with post-hoc Newman Keuls comparison test; control versus DEAB plus RA, $P < 0.01$; control versus DEAB plus sulpiride, $P < 0.01$) and for oEPSC (control, 109.20 ± 13.28 pA, n = 17 cells; DEAB plus RA, 94.51 ± 17.17 pA, n = 5 cells; DEAB plus sulpiride, 147 ± 18.89 pA, n = 11 cells; $F_{2, 30} = 2.139$, $P > 0.05$, one-way ANOVA). Data used for control group are the same control used in Fig. 2F. Blue rectangular bar indicates 450 nm light stimulation. Scale bars represent 400 pA, 100 ms for oIPSC and 50 pA, 100 ms for oEPSC. Mean ± SEM is used for all the data described in the figure. **P < 0.01.

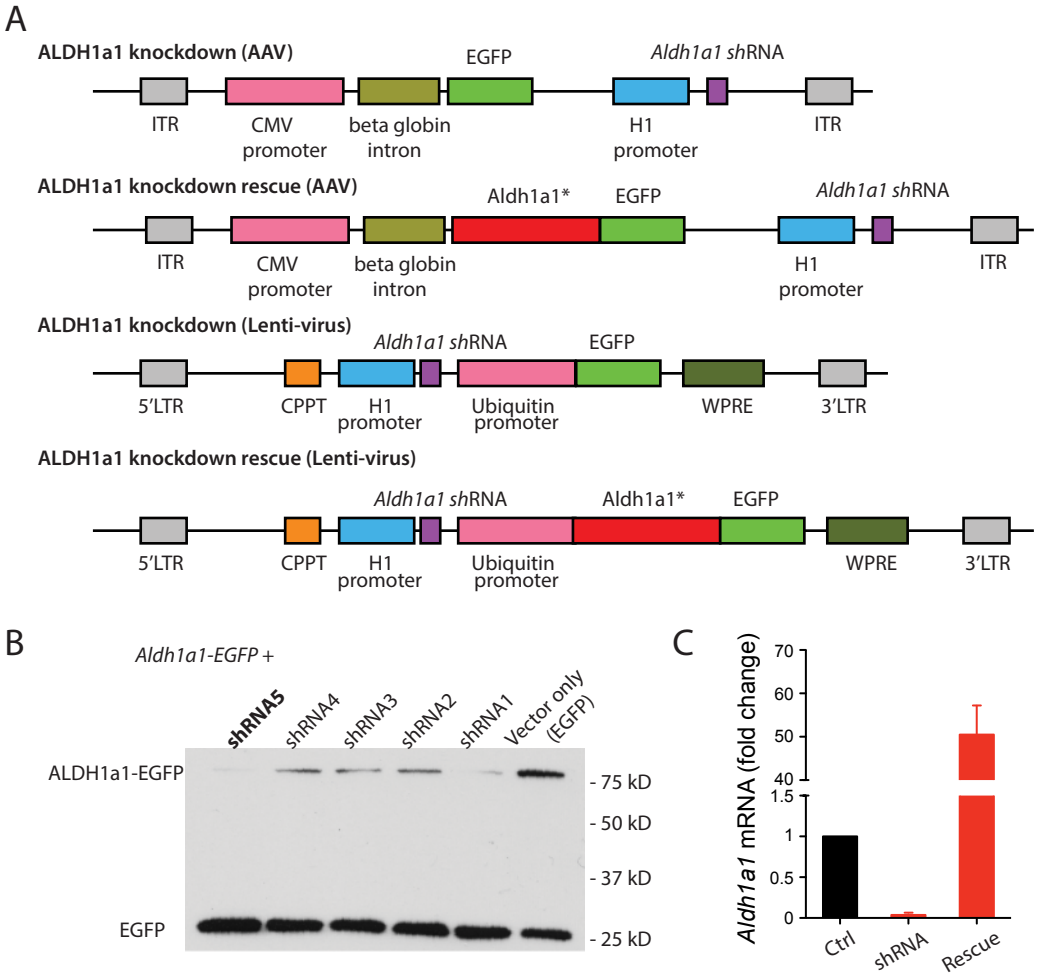

fig. S9. *Aldh1a1* shRNA knockdown and rescue.

(A) Schematized lentiviral or AAV vectors for expression of shRNA and EGFP or Aldh1a1*-EGFP. Aldh1a1* indicates an shRNA-resistant wild-type Aldh1a1. (B) HEK293 cells were transfected with 0.5 μg of aldh1a1-GFP construct and 1.5 μg of shRNA construct and expressed for 24 hours. Lysates were separated by SDS-PAGE and immunoblotted with anti-GFP antibody. shRNA-5 had the strongest knock-down and was utilized for subsequent in vivo experiments. (C) Dissociated culture of mouse hippocampal neurons infected with lentivirus containing shRNA against *Aldh1a1* (shRNA-5 from blot in B), shRNA rescue construct or empty vector, were analyzed by qRTPCR for *Aldh1a1*. Relative expression of *Aldh1a1* clearly demonstrates efficient shRNA-mediated *Aldh1a1* loss. Mean ± SEM is used for all the data described in the figure.

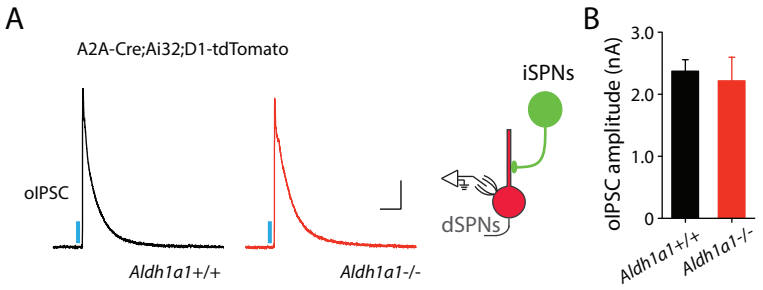

fig. S10. Conventional GABA transmission is not altered in *Aldh1a1*-/- mice.
(A) Representative oIPSC traces recorded from *Aldh1a1*+/+;A2A-Cre;Ai32;Drd1a-tdTomato (left) or *Aldh1a1*-/-;A2A-Cre;Ai32;Drd1a-tdTomato (right) mice. (B) Summary statistics for oIPSC (*Aldh1a1*+/+, 2.37 ± 0.18 nA, n = 5 cells; *Aldh1a1*-/-, 2.22 ± 0.38 nA, n = 8 cells; P > 0.05, unpaired t-test). Blue rectangular bar in-dicates 450 nm light stimulation. Scale bars represent 400 pA, 100 ms for oIPSC. Mean ± SEM is used for all the data described in the figure.

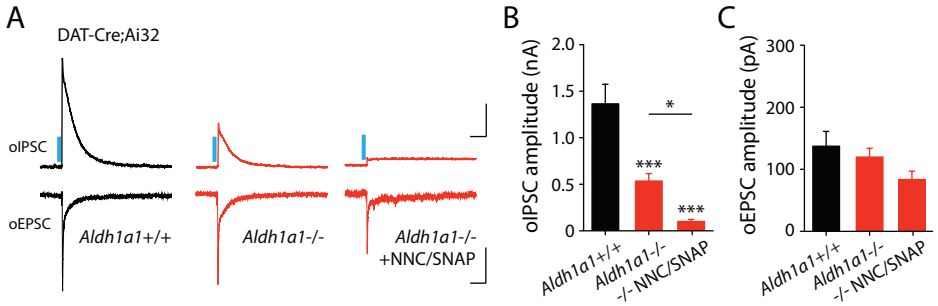

fig. S11. Combination of GABA transporter GAT1 and GAT3 blockers abolish residual dopaminergic oIPSC in *Aldh1a1*-/- mice.
(A) Representative oIPSC and oEPSC recording traces in *Aldh1a1*+/+;DAT-Cre;Ai32 or *Aldh1a1*-/-;DAT-Cre;Ai32 mice, treated with NNC-711 (4 μM) plus SNAP-5114 (50 μM). (B) Summary statistics for oIPSC (A*ldh1a1*+/+, 1.37 ± 0.21 nA, n = 9 cells; A*ldh1a1*-/-, 0.54 ± 0.08 nA, n = 10 cells; A*ldh1a1*-/- treated with NNC-711 plus SNAP-5114, 0.10 ± 0.02 nA, n = 10 cells; $F_{2, 26} = 26.48$, P < 0.0001, one-way ANOVA with post-hoc Newman Keuls comparison test; A*ldh1a1*+/+ vs A*ldh1a1*-/-, P < 0.001; *Aldh1a1*+/+ vs *Aldh1a1*-/- with NNC-711 plus SNAP-5114, P < 0.001; *Aldh1a1*-/- vs *Aldh1a1*-/- with NNC-711 plus SNAP-5114, P < 0.05). (C) Summary statistics for oEPSC (*Aldh1a1*+/+, 137.30 ± 23.96 pA, n = 8 cells; A*ldh1a1*-/-, 119.90 ± 14.09 pA, n = 9 cells; A*ldh1a1*-/- treated with NNC-711 plus SNAP-5114, 83.65 ± 13.40 pA, n = 8 cells; $F_{2, 22} = 2.338$, P > 0.05, one-way ANOVA). Data used for *Aldh1a1*+/+ and *Aldh1a1*-/- groups are the same as used in Fig. 3E-G. Blue rectangular bar indicates 450 nm light stimulation. Scale bars represent 400 pA, 100 ms for oIPSC and 50 pA, 100 ms for oEPSC. Mean ± SEM is used for all the data described in the figure.

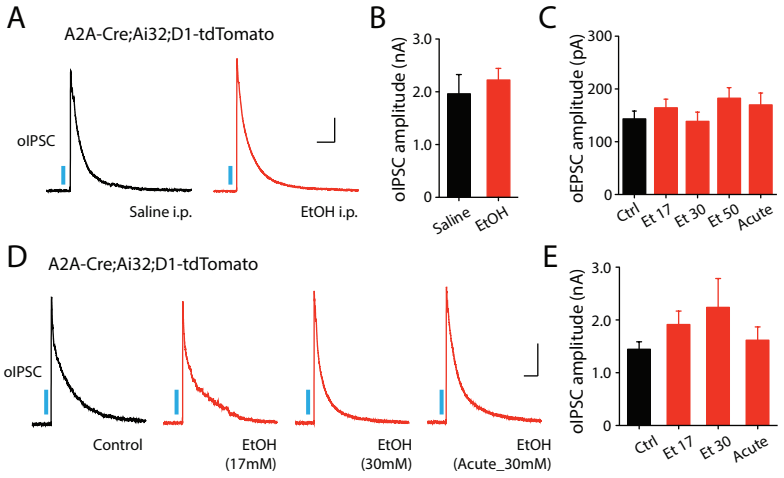

fig. S12. GABAergic inputs from iSPNs to dSPNs are not affected by ethanol treatments in vivo or in vitro.

(A) Representative oIPSC recording traces in A2A-Cre;Ai32;Drd1a-tdTomato mice injected with either saline or EtOH (2 g/kg, once a day, i.p.) for 7 consecutive days. (B) Summary statistics for oIPSC (saline, 1.96 ± 0.37 nA, n = 12 cells; EtOH, 2.22 ± 0.22 nA, n = 13 cells; $P > 0.05$, un-paired t-test). (C) Summary statistics for oEPSC in DAT-Cre;Ai32 mice incubated and bath-applied with different concentrations of ethanol (17, 30, and 50 mM) (control, 143.20 ± 14.91 pA, n = 14 cells; EtOH 17 mM, 164.40 ± 16.28 pA, n = 11 cells; EtOH 30 mM, 138.70 ± 17.45 pA, n = 12 cells; EtOH 50 mM, 182.60 ± 19.89 pA, n = 10 cells; acute EtOH 30 mM, 169.90 ± 22.44 pA, n = 9 cells; $F_{4, 51} = 1.072$, $P > 0.05$, one-way ANOVA). (D) Representative oIPSC recording traces in A2A-Cre;Ai32;Drd1a-tdTomato mice incubated and bath-applied with ethanol (17 and 30 mM). (E) Summary statistics for oIPSC (control, 1.45 ± 0.14 nA, n = 14 cells; EtOH 17 mM, 1.91 ± 0.26 nA, n = 12 cells; EtOH 30 mM, 2.24 ± 0.55 nA, n = 10 cells; acute EtOH 30 mM, 1.62 ± 0.25 nA, n = 10 cells; $F_{3, 42} = 1.288$, $P > 0.05$, one-way ANOVA). Blue rectangular bar in-dicates 450 nm light stimulation. Scale bars represent 400 pA, 100 ms for oIPSC. Error bars indicate Mean ± SEM throughout the figure.

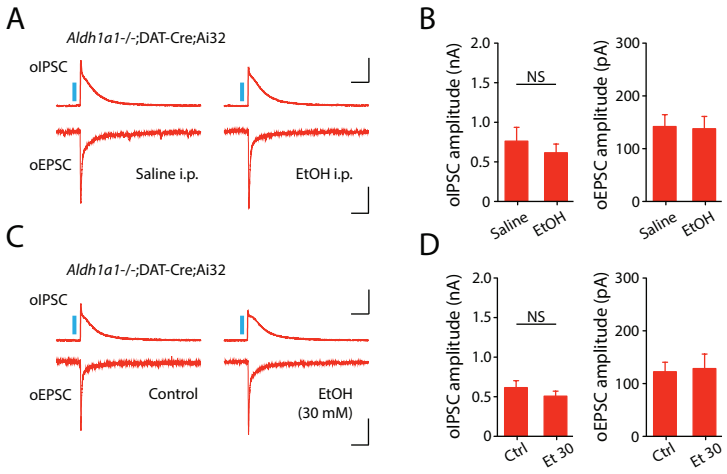

fig. S13. Modulation of GABA co-release by ethanol requires ALDH1a1.
(A) Representative oIPSC and oEPSC recording traces in *Aldh1a1*-/-;DAT-Cre;Ai32 mice injected with saline or EtOH (2 g/kg, 20%, once a day, i.p.) for 7 consecutive days. (B) Summary statistics for oIPSC (control, 0.76 ± 0.17 nA, n = 7 cells; EtOH, 0.61 ± 0.11 nA, n = 14 cells; P > 0.05, unpaired t-test) and oEPSC (control, 142.10 ± 22.43 pA, n = 6 cells; EtOH, 137.80 ± 23.40 pA, n = 12 cells; P > 0.05, unpaired t-test). (C) Representative oIPSC and oEPSC recording traces in *Aldh1a1*-/-;DAT-Cre;Ai32 mice treated with EtOH (30 mM). (D) Summary statistics for oIPSC (control, 0.62 ± 0.09 nA, n = 10 cells; EtOH, 0.51 ± 0.06 nA, n = 7 cells; P > 0.05, unpaired t-test) and oEPSC (control, 122.50 ± 17.96 pA, n = 7 cells; EtOH, 128.50 ± 27.62 pA, n = 6 cells; P > 0.05, unpaired t-test). Blue rectangular bar indicates 450 nm light stimulation. Scale bars represent 400 pA, 100 ms for oIPSC and 50 pA, 100 ms for oEPSC. Error bars indicate Mean ± SEM throughout the figure.

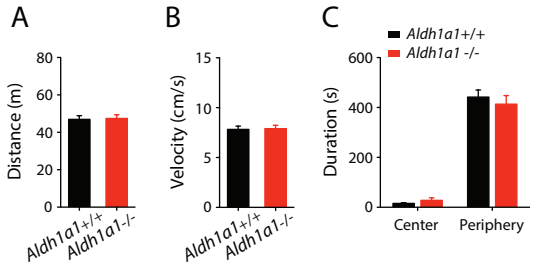

fig. S14. Basal locomotion is not impaired in *Aldh1a1*-/- mice.
(A) Total ambulatory distance during open field test (*Aldh1a1*+/+, 46.92 ± 1.98 m, n = 8 mice; *Aldh1a1*-/-, 47.42 ± 1.98 m, n = 11 mice; P > 0.05, unpaired t-test). (B) Ambulatory velocity during open field test (*Aldh1a1*+/+, 7.83 ± 0.33 cm/s, n = 8 mice; *Aldh1a1*-/-, 7.90 ± 0.33 cm/s, n = 11 mice; P > 0.05, unpaired t-test). (C) Total time spent in each area of arena (center and periphery) during open field test (center, *Aldh1a1*+/+, 15.55 ± 2.81 s, n = 8 mice; *Aldh1a1*-/-, 28.00 ± 9.75 s, n = 11 mice; periphery, *Aldh1a1*+/+, 441.80 ± 28.28 s, n = 8 mice; *Aldh1a1*-/-, 413.30 ± 34.65 s, n = 11 mice; repeated measures 2-way ANOVA, genotype effect, $F_{1, 17} = 0.151$, P > 0.05, arena location effect, $F_{1, 17} = 215.5$, P < 0.0001, interaction, $F_{1, 17} = 0.550$, P > 0.05). Mean ± SEM is used for all the data described in the figure.

FIGURE		DESCRIPTION	VALUE	N number	STATISTIC	P VALUE	POST TEST	POST TEST P VALUE
1	A-J	SAMPLE IMAGE	N/A	N/A	N/A	N/A	N/A	N/A
	K(left, SNc)	*Gad1*+:TH+/Total TH+ neurons	8.7 ± 0.9 %	704 cells	N/A	N/A	N/A	N/A
	K(left, SNc)	*Gad2*+:TH+/Total TH+ neurons	8.8 ± 1.0 %	660 cells, 12 slices, 3 mice	N/A	N/A	N/A	N/A
	K(right, VTA	*Gad1*+:TH+/Total TH+ neurons	13.8 ± 3.2 %	377 cells	N/A	N/A	N/A	N/A
	K(right, VTA	*Gad2*+:TH+/Total TH+ neurons	18.4 ± 5.6 %	353 cells, 12 slices, 3 mice	N/A	N/A	N/A	N/A
	L	CONTROL	1.32 ± 0.19 nA	7 cells	F(2, 15) = 16.79 (1-way ANOVA)	0.0001	CONTROL VS 3-MPA	< 0.01
		3-MPA (500 µM)	0.56 ± 0.2 nA	5 cells			CONTROL VS *Gad1* fl/fl;*Gad2* fl/fl	< 0.001
		Gad1 fl/fl;*Gad2* fl/fl	0.07 ± 0.01 nA	6 cells			Newman Keuls	
	M	SAMPLE TRACE	N/A	N/A	N/A	N/A	N/A	N/A
	N	CONTROL (oIPSC)	1.08 ± 0.14 nA	6 cells	t(10) = 0.015 (Unpaired t-test)	> 0.05	N/A	N/A
		3-MPA (oIPSC) (500 µM)	1.08 ± 0.18 nA	6 cells				
		CONTROL (oEPSC)	109.70 ± 10.80 pA	6 cells	t(10) = 0.821 (Unpaired t-test)	> 0.05	N/A	N/A
		3-MPA (oEPSC) (500 µM)	144 ± 40.29 pA	6 cells				
	O	SAMPLE TRACE	N/A	N/A	N/A	N/A	N/A	N/A
	P	+/+ (oIPSC)	1.22 ± 0.09 nA	10 cells	t(15) = 0.826 (Unpaired t-test)	> 0.05	N/A	N/A
		fl/fl (oIPSC)	1.35 ± 0.12 nA	7 cells				
		+/+ (oEPSC)	157.10 ± 25.35 pA	8 cells	t(12) = 0.119 (Unpaired t-test)	> 0.05	N/A	N/A
		fl/fl (oEPSC)	162.30 ± 39.09 pA	6 cells				
2	A B	SAMPLE IMAGE	N/A	N/A	N/A	N/A	N/A	N/A
	C(SNc)	ALDH1a1+:TH+/Total TH+ neurons	74.8 ± 3.9 %	337 cells, 11 slices, 2 mice	N/A	N/A	N/A	N/A
	C(VTA)	ALDH1a1+:TH+/Total TH+ neurons	26.8 ± 2.4 %	399 cells, 7 slices, 2 mice	N/A	N/A	N/A	N/A
	D	SAMPLE IMAGE	N/A	N/A	N/A	N/A	N/A	N/A
	E	SAMPLE TRACE	N/A	N/A	N/A	N/A	N/A	N/A
	F	CONTROL (oIPSC)	1.27 ± 0.16 nA	17 cells	t(27) = 3.708 (Unpaired t-test)	0.001	N/A	N/A
		DEAB (oIPSC) (10 µM)	0.54 ± 0.08 nA	12 cells				
		CONTROL (oEPSC)	109.20 ± 13.28 pA	17 cells	t(27) = 1.132 (Unpaired t-test)	> 0.05	N/A	N/A
		DEAB (oEPSC) (10 µM)	143.10 ± 30.54 pA	12 cells				
	G	SAMPLE TRACE	N/A	N/A	N/A	N/A	N/A	N/A
	H	CONTROL (oIPSC)	1.16 ± 0.11 nA	12 cells	t(22) = 4.261 (Unpaired t-test)	< 0.001	N/A	N/A
		Aminoguanidine (oIPSC) (100 µM)	0.52 ± 0.10 nA	12 cells				
		CONTROL (oEPSC)	87.62 ± 13.65 pA	11 cells	t(17) = 0.479 (Unpaired t-test)	> 0.05	N/A	N/A
		Aminoguanidine (oEPSC) (100 µM)	76.63 ± 19.26 pA	8 cells				
3	A	KD and rescue viral construct map						
	B	SAMPLE IMAGE	N/A	N/A	N/A	N/A	N/A	N/A
	C	SAMPLE TRACE	N/A	N/A		N/A	N/A	N/A
	D	CONTROL virus (oIPSC)	1.06 ± 0.13 nA	14 cells	F(2, 32) = 5.174 (1-way ANOVA)	< 0.05	CONTROL virus VS KD	< 0.01
		KD (oIPSC)	0.61 ± 0.08 nA	11 cells			KD VS Rescue	< 0.05
		Rescue (oIPSC)	1.07 ± 0.12 nA	10 cells			Newman Keuls	
		CONTROL virus (oEPSC)	116.40 ± 13.39 pA	12 cells	F(2, 28) = 0.799 (1-way ANOVA)	> 0.05	N/A	N/A
		KD (oEPSC)	95.37 ± 11.44 pA	10 cells				
		Rescue (oEPSC)	113.10 ± 12.50 pA	9 cells				
	E	SAMPLE TRACE	N/A	N/A	N/A	N/A	N/A	N/A
	F	*Aldh1a1*+/+ (oIPSC)	1.37 ± 0.21 nA	9 cells	F(3, 35) = 10.53 (1-way ANOVA)	< 0.0001	*Aldh1a1*+/+ VS *Aldh1a1*-/-	< 0.001
		Aldh1a1-/- (oIPSC)	0.54 ± 0.08 nA	10 cells			*Aldh1a1*+/+ VS *Aldh1a1*-/- plus DEAB	< 0.001
		Aldh1a1-/- plus DEAB (oIPSC) (10 µM)	0.51 ± 0.08 nA	10 cells			*Aldh1a1*+/+ VS *Aldh1a1*-/- plus AG	< 0.001
		Aldh1a1-/- plus AG (oIPSC) (100 µM)	0.69 ± 0.08 nA	10 cells			Newman Keuls	
	G	*Aldh1a1*+/+ (oEPSC)	137.30 ± 23.96 pA	8 cells	F(3, 33) = 0.607 (1-way ANOVA)	> 0.05	N/A	N/A
		Aldh1a1-/- (oEPSC)	119.90 ± 14.09 pA	9 cells				
		Aldh1a1-/- plus DEAB (oEPSC) (10 µM)	149.60 ± 15.30 pA	10 cells				
		Aldh1a1-/- plus AG (oEPSC) (100 µM)	143 ± 12.92 nA	10 cells				
	H	SAMPLE TRACE	N/A	N/A	N/A	N/A	N/A	N/A
	I	*Aldh1a1*-/- plus CONTROL virus (oIPSC)	0.60 ± 0.06 nA	12 cells	t(22) = 2.089 (Unpaired t-test)	< 0.05	N/A	N/A
		Aldh1a1-/- plus Rescue (oIPSC)	0.91 ± 0.13 nA	12 cells				
		Aldh1a1-/- plus CONTROL virus (oEPSC)	131.40 ± 15.38 pA	10 cells	t(19) = 0.565 (Unpaired t-test)	> 0.05	N/A	N/A
		Aldh1a1-/- plus Rescue (oEPSC)	119.50 ± 14.33 pA	11 cells				
4	A	SAMPLE TRACE	N/A	N/A	N/A	N/A	N/A	N/A
	B	CONTROL saline (oIPSC)	1.49 ± 0.17 nA	13 cells	t(25) = 4.810 (Unpaired t-test)	< 0.0001	N/A	N/A
		EtOH CIE (oIPSC)	0.63 ± 0.08 nA	14 cells				
		CONTROL saline (oEPSC)	181.30 ± 19.33 pA	9 cells	t(20) = 1.483 (Unpaired t-test)	> 0.05	N/A	N/A
		EtOH CIE (oEPSC)	136.30 ± 21.35 pA	13 cells				
	C	SAMPLE TRACE	N/A	N/A	N/A	N/A	N/A	N/A
	D	CONTROL (oIPSC)	1.36 ± 0.12 nA	14 cells	F(4, 57) = 7.052 (1-way ANOVA)	0.001	CONTROL VS EtOH 30 mM	< 0.01
		EtOH 17 mM (oIPSC)	1.08 ± 0.13 nA	13 cells			CONTROL VS EtOH 50 mM	< 0.001
		EtOH 30 mM (oIPSC)	0.72 ± 0.08 nA	14 cells			EtOH 17 mM VS EtOH 30 mM	< 0.05
		EtOH 50 mM (oIPSC)	0.62 ± 0.08 nA	12 cells			EtOH 17 mM VS EtOH 50 mM	< 0.05
		EtOH acute 30 mM (oIPSC)	1.24 ± 0.21 nA	9 cells			EtOH 30 mM VS acute EtOH 30 mM	< 0.05
							EtOH 50 mM VS acute EtOH 30 mM	< 0.01
	E	Behavior protocol	N/A	N/A	N/A	N/A	N/A	N/A
	F	*Aldh1a1*+/+ (3%)	2.35 ± 0.21 g/kg/day	9 mice per each genotype	Repeated measures 2-way ANOVA			
		Aldh1a1-/- (3%)	2.92 ± 0.18 g/kg/day		Interation (F(1, 16) = 9.930)	< 0.01	*Aldh1a1*+/+ VS *Aldh1a1*-/- (3% EtOH)	> 0.05
		Aldh1a1+/+ (10%)	7.00 ± 1.24 g/kg/day		EtOH concentraion effect (F(1, 16) = 97.80)	< 0.0001	*Aldh1a1*+/+ VS *Aldh1a1*-/- (10% EtOH)	< 0.001
		Aldh1a1-/- (10%)	11.92 ± 0.57 g/kg/day		Genotype effect (F(1, 16) = 15.220)	< 0.01	Bonferroni	
	G	*Aldh1a1*+/+ (3%)	53.88 ± 10.04 ml/kg/day	9 mice per each genotype	Repeated measures 2-way ANOVA			
		Aldh1a1-/- (3%)	52.56 ± 5.11 ml/kg/day		Interation (F(1, 16) = 0.439)	> 0.05		
		Aldh1a1+/+ (10%)	43.00 ± 7.37 ml/kg/day		EtOH concentraion effect (F(1, 16) = 9.920)	< 0.01	N/A	
		Aldh1a1-/- (10%)	35.89 ± 2.76 ml/kg/day		Genotype effect (F(1, 16) = 0.237)	> 0.05		
	H	*Aldh1a1*+/+ (3%)	54.03 ± 1.94 %	9 mice per each genotype	Repeated measures 2-way ANOVA			
		Aldh1a1-/- (3%)	56.78 ± 1.81 %		Interation (F(1, 16) = 4.146)	> 0.05	*Aldh1a1*+/+ VS *Aldh1a1*-/- (3% EtOH)	> 0.05
		Aldh1a1+/+ (10%)	57.40 ± 2.64 %		EtOH concentraion effect (F(1, 16) = 19.930)	< 0.001	*Aldh1a1*+/+ VS *Aldh1a1*-/- (10% EtOH)	< 0.05
		Aldh1a1-/- (10%)	65.80 ± 1.69 %		Genotype effect (F(1, 16) = 4.791)	< 0.05	Bonferroni	
	I	Control virus (3%)	2.81 ± 0.40 g/kg/day	10 mice	Repeated measures 2-way ANOVA			
		Aldh1a1 KD virus (3%)	3.02 ± 0.31 g/kg/day	10 mice	Interation (F(2, 26) = 16.690)	< 0.0001		
		Rescue virus (3%)	2.23 ± 0.13 g/kg/day	9 mice	EtOH concentraion effect (F(1, 26) = 178.80)	< 0.0001	Control virus VS *Aldh1a1* KD virus (10% EtOH)	< 0.001
		Control virus (10%)	8.89 ± 1.19 g/kg/day	(same mice as above)	Genotype effect (F(2, 16) = 14.540)	< 0.0001	*Aldh1a1* KD virus VS Rescue virus (10% EtOH)	< 0.001
		Aldh1a1 KD virus (10%)	14.69 ± 1.16 g/kg/day	(same mice as above)				
		Rescue virus (10%)	6.46 ± 0.54 g/kg/day	(same mice as above)			Bonferroni	
	J	Control virus (3%)	72.39 ± 10.67 ml/kg/day	10 mice	Repeated measures 2-way ANOVA			
		Aldh1a1 KD virus (3%)	80.57 ± 8.71 ml/kg/day	10 mice	Interation (F(2, 26) = 1.424)	> 0.05		
		Rescue virus (3%)	61.14 ± 3.42 ml/kg/day	9 mice	EtOH concentraion effect (F(1, 26) = 30.760)	< 0.0001		
		Control virus (10%)	50.45 ± 4.64 ml/kg/day	(same mice as above)	Genotype effect (F(2, 16) = 0.845)	> 0.05		
		Aldh1a1 KD virus (10%)	52.27 ± 6.08 ml/kg/day	(same mice as above)			N/A	
		Rescue virus (10%)	48.54 ± 4.97 ml/kg/day	(same mice as above)				
	K	Control virus (3%)	53.15 ± 1.76 %	10 mice	Repeated measures 2-way ANOVA			
		Aldh1a1 KD virus (3%)	52.93 ± 1.26 %	10 mice	Interation (F(2, 26) = 7.059)	< 0.01		
		Rescue virus (3%)	54.69 ± 0.59 %	9 mice	EtOH concentraion effect (F(1, 26) = 40.480)	< 0.0001	Control virus VS *Aldh1a1* KD virus (10% EtOH)	< 0.01
		Control virus (10%)	57.30 ± 1.92 %	(same mice as above)	Genotype effect (F(2, 16) = 1.840)	> 0.05	*Aldh1a1* KD virus VS Rescue virus (10% EtOH)	< 0.05
		Aldh1a1 KD virus (10%)	64.18 ± 1.80 %	(same mice as above)				
		Rescue virus (10%)	57.79 ± 1.17 %	(same mice as above)			Bonferroni	

Table S1

All values and statistics for Fig. 1 to 4

REFERENCES

1. W. Schultz, Multiple dopamine functions at different time courses. *Annual review of neuroscience* **30**, 259 (2007).
2. N. X. Tritsch, B. L. Sabatini, Dopaminergic modulation of synaptic transmission in cortex and striatum. *Neuron* **76**, 33 (Oct 4, 2012).
3. B. T. Chen, F. W. Hopf, A. Bonci, Synaptic plasticity in the mesolimbic system: therapeutic implications for substance abuse. *Annals of the New York Academy of Sciences* **1187**, 129 (Feb, 2010).
4. P. Redgrave *et al.*, Goal-directed and habitual control in the basal ganglia: implications for Parkinson's disease. *Nature reviews. Neuroscience* **11**, 760 (Nov, 2010).
5. N. X. Tritsch, J. B. Ding, B. L. Sabatini, Dopaminergic neurons inhibit striatal output through non-canonical release of GABA. *Nature* **490**, 262 (Oct 11, 2012).
6. T. Gonzalez-Hernandez, P. Barroso-Chinea, A. Acevedo, E. Salido, M. Rodriguez, Colocalization of tyrosine hydroxylase and GAD65 mRNA in mesostriatal neurons. *The European journal of neuroscience* **13**, 57 (Jan, 2001).
7. N. X. Tritsch, W. J. Oh, C. Gu, B. L. Sabatini, Midbrain dopamine neurons sustain inhibitory transmission using plasma membrane uptake of GABA, not synthesis. *eLife* **3**, e01936 (2014).
8. W. Matsuda *et al.*, Single nigrostriatal dopaminergic neurons form widely spread and highly dense axonal arborizations in the neostriatum. *The Journal of neuroscience : the official journal of the Society for Neuroscience* **29**, 444 (Jan 14, 2009).
9. C. L. Heusner, L. R. Beutler, C. R. Houser, R. D. Palmiter, Deletion of GAD67 in dopamine receptor-1 expressing cells causes specific motor deficits. *Genesis* **46**, 357 (Jul, 2008).
10. S. Lammel *et al.*, Diversity of transgenic mouse models for selective targeting of midbrain dopamine neurons. *Neuron* **85**, 429 (Jan 21, 2015).
11. P. Hoerbelt, T. A. Lindsley, M. W. Fleck, Dopamine directly modulates GABAA receptors. *The Journal of neuroscience : the official journal of the Society for Neuroscience* **35**, 3525 (Feb 25, 2015).
12. K. Williams, Modulation and block of ion channels: a new biology of polyamines. *Cellular signalling* **9**, 1 (Jan, 1997).
13. S. G. Xing, Y. B. Jun, Z. W. Hau, L. Y. Liang, Higher accumulation of gamma-aminobutyric acid induced by salt stress through stimulating the activity of diamine oxidases in Glycine max (L.) Merr. roots. *Plant physiology and biochemistry : PPB / Societe francaise de physiologie vegetale* **45**, 560 (Aug, 2007).
14. B. J. Shelp *et al.*, Hypothesis/review: contribution of putrescine to 4-aminobutyrate (GABA) production in response to abiotic stress. *Plant science : an international journal of experimental plant biology* **193-194**, 130 (Sep, 2012).
15. M. R. Bell, J. A. Belarde, H. F. Johnson, C. D. Aizenman, A neuroprotective role for polyamines in a Xenopus tadpole model of epilepsy. *Nature neuroscience* **14**, 505 (Apr, 2011).
16. E. B. Sequerra, P. Gardino, C. Hedin-Pereira, F. G. de Mello, Putrescine as an important source of GABA in the postnatal rat subventricular zone. *Neuroscience* **146**, 489 (May 11, 2007).
17. T. Noto *et al.*, The effect of L-erythro-dihydroxyphenylserine injected into the lateral ventricle and the hypothalamus on the locomotor activity. *Pharmacology, biochemistry,*

and behavior **25**, 411 (Aug, 1986).
18. E. N. Yamasaki, V. D. Barbosa, F. G. De Mello, J. N. Hokoc, GABAergic system in the developing mammalian retina: dual sources of GABA at early stages of postnatal development. *International journal of developmental neuroscience : the official journal of the International Society for Developmental Neuroscience* **17**, 201 (Jun, 1999).
19. J. Laschet, T. Grisar, M. Bureau, D. Guillaume, Characteristics of putrescine uptake and subsequent GABA formation in primary cultured astrocytes from normal C57BL/6J and epileptic DBA/2J mouse brain cortices. *Neuroscience* **48**, 151 (1992).
20. B. A. Barres, W. J. Koroshetz, K. J. Swartz, L. L. Chun, D. P. Corey, Ion channel expression by white matter glia: the O-2A glial progenitor cell. *Neuron* **4**, 507 (Apr, 1990).
21. J. Aoto, C. I. Nam, M. M. Poon, P. Ting, L. Chen, Synaptic signaling by all-trans retinoic acid in homeostatic synaptic plasticity. *Neuron* **60**, 308 (Oct 23, 2008).
22. G. Liu *et al.*, Aldehyde dehydrogenase 1 defines and protects a nigrostriatal dopaminergic neuron subpopulation. *The Journal of clinical investigation* **124**, 3032 (Jul, 2014).
23. P. McCaffery, U. C. Drager, High levels of a retinoic acid-generating dehydrogenase in the meso-telencephalic dopamine system. *Proceedings of the National Academy of Sciences of the United States of America* **91**, 7772 (Aug 2, 1994).
24. V. Vasiliou, A. Pappa, D. R. Petersen, Role of aldehyde dehydrogenases in endogenous and xenobiotic metabolism. *Chemico-biological interactions* **129**, 1 (Dec 1, 2000).
25. D. S. Goldstein *et al.*, Determinants of buildup of the toxic dopamine metabolite DOPAL in Parkinson's disease. *Journal of neurochemistry* **126**, 591 (Sep, 2013).
26. X. Fan *et al.*, Targeted disruption of Aldh1a1 (Raldh1) provides evidence for a complex mechanism of retinoic acid synthesis in the developing retina. *Molecular and cellular biology* **23**, 4637 (Jul, 2003).
27. R. Sherva *et al.*, Associations and interactions between SNPs in the alcohol metabolizing genes and alcoholism phenotypes in European Americans. *Alcoholism, clinical and experimental research* **33**, 848 (May, 2009).
28. J. Liu *et al.*, Haplotype-based study of the association of alcohol-metabolizing genes with alcohol dependence in four independent populations. *Alcoholism, clinical and experimental research* **35**, 304 (Feb, 2011).
29. B. J. Everitt, T. W. Robbins, Neural systems of reinforcement for drug addiction: from actions to habits to compulsion. *Nature neuroscience* **8**, 1481 (Nov, 2005).
30. G. Chen *et al.*, Striatal involvement in human alcoholism and alcohol consumption, and withdrawal in animal models. *Alcoholism, clinical and experimental research* **35**, 1739 (Oct, 2011).
31. J. Wang *et al.*, Ethanol-mediated facilitation of AMPA receptor function in the dorsomedial striatum: implications for alcohol drinking behavior. *The Journal of neuroscience : the official journal of the Society for Neuroscience* **32**, 15124 (Oct 24, 2012).
32. L. E. O'Dell, A. J. Roberts, R. T. Smith, G. F. Koob, Enhanced alcohol self-administration after intermittent versus continuous alcohol vapor exposure. *Alcoholism, clinical and experimental research* **28**, 1676 (Nov, 2004).
33. S. Ben Hamida *et al.*, Protein tyrosine phosphatase alpha in the dorsomedial striatum promotes excessive ethanol-drinking behaviors. *The Journal of neuroscience : the official*

journal of the Society for Neuroscience **33**, 14369 (Sep 4, 2013).
34. T. S. Hnasko *et al.*, Vesicular glutamate transport promotes dopamine storage and glutamate corelease in vivo. *Neuron* **65**, 643 (Mar 11, 2010).
35. D. H. Root *et al.*, Single rodent mesohabenular axons release glutamate and GABA. *Nature neuroscience* **17**, 1543 (Nov, 2014).
36. S. J. Shabel, C. D. Proulx, J. Piriz, R. Malinow, Mood regulation. GABA/glutamate co-release controls habenula output and is modified by antidepressant treatment. *Science* **345**, 1494 (Sep 19, 2014).
37. D. M. Lovinger, Neurotransmitter roles in synaptic modulation, plasticity and learning in the dorsal striatum. *Neuropharmacology* **58**, 951 (Jun, 2010).
38. C. M. Pennartz *et al.*, Corticostriatal Interactions during Learning, Memory Processing, and Decision Making. *The Journal of neuroscience : the official journal of the Society for Neuroscience* **29**, 12831 (Oct 14, 2009).
39. J. L. Weiner, C. F. Valenzuela, Ethanol modulation of GABAergic transmission: the view from the slice. *Pharmacology & therapeutics* **111**, 533 (Sep, 2006).
40. L. Madisen *et al.*, A toolbox of Cre-dependent optogenetic transgenic mice for light-induced activation and silencing. *Nature neuroscience* **15**, 793 (May, 2012).
41. J. Ding, J. D. Peterson, D. J. Surmeier, Corticostriatal and thalamostriatal synapses have distinctive properties. *The Journal of neuroscience : the official journal of the Society for Neuroscience* **28**, 6483 (Jun 18, 2008).
42. A. S. Bryant, B. Li, M. P. Beenhakker, J. R. Huguenard, Maintenance of thalamic epileptiform activity depends on the astrocytic glutamate-glutamine cycle. *Journal of neurophysiology* **102**, 2880 (Nov, 2009).
43. S. Gong *et al.*, Targeting Cre recombinase to specific neuron populations with bacterial artificial chromosome constructs. *The Journal of neuroscience : the official journal of the Society for Neuroscience* **27**, 9817 (Sep 12, 2007).
44. L. Heja *et al.*, Astrocytes convert network excitation to tonic inhibition of neurons. *BMC biology* **10**, 26 (2012).
45. V. Koppaka *et al.*, Aldehyde dehydrogenase inhibitors: a comprehensive review of the pharmacology, mechanism of action, substrate specificity, and clinical application. *Pharmacological reviews* **64**, 520 (Jul, 2012).
46. M. E. Soden, L. Chen, Fragile X protein FMRP is required for homeostatic plasticity and regulation of synaptic strength by retinoic acid. *The Journal of neuroscience : the official journal of the Society for Neuroscience* **30**, 16910 (Dec 15, 2010).
47. W. Xu *et al.*, Distinct neuronal coding schemes in memory revealed by selective erasure of fast synchronous synaptic transmission. *Neuron* **73**, 990 (Mar 8, 2012).
48. S. Zolotukhin *et al.*, Recombinant adeno-associated virus purification using novel methods improves infectious titer and yield. *Gene therapy* **6**, 973 (Jun, 1999).
49. S. Carnicella, D. Ron, S. Barak, Intermittent ethanol access schedule in rats as a preclinical model of alcohol abuse. *Alcohol* **48**, 243 (May, 2014).
50. T. J. Phillips *et al.*, Alcohol preference and sensitivity are markedly reduced in mice lacking dopamine D2 receptors. *Nature neuroscience* **1**, 610 (Nov, 1998).